

SYNTHESIS AND CRYSTAL STRUCTURE OF NEW HYDRATED LEAD SELENITE NITRATE

$\text{Pb}_4(\text{SeO}_3)_3(\text{NO}_3)_2 \cdot 2\text{H}_2\text{O}$

O. I. Siidra^{1,2*} and V. Yu. Grishaev¹

The synthesis and crystal structure of new hydrated lead selenite nitrate $\text{Pb}_4(\text{SeO}_3)_3(\text{NO}_3)_2 \cdot 2\text{H}_2\text{O}$ (**1**) are reported. The crystal structure of **1** ($P\bar{1}$, $a = 7.2590(2)$ Å, $b = 7.6454(2)$ Å, $c = 14.7293(4)$ Å, $\alpha = 84.386(2)^\circ$, $\beta = 78.311(2)^\circ$, $\gamma = 83.643(2)^\circ$, $V = 793.18(4)$ Å³, $R_1 = 3.1\%$) belongs to a new structure type. It is based on a porous framework composed of $[\text{Pb}_4(\text{SeO}_3)_3]^{2+}$ layers strongly bound via nitrate anions. Water molecules are located in the channels. Stereochemically active electron pairs of SeO_3E groups are directed toward each other. The structure of **1** is compared with similar architectures involving Pb^{2+} and Se^{4+} cations.

DOI: 10.1134/S002247662407014X

Keywords: lead, selenites, nitrates, inorganic synthesis.

INTRODUCTION

The use of non-transition metal cations in low oxidation states is one of the tools for the targeted synthesis of compounds with low-dimensional crystal structures due to the stereochemical activity of lone pairs. In particular, among such compounds there are many representatives with non-centrosymmetric and low-dimensional structures. The formation probability of these structures increases when a halogen anion is incorporated into them [1]. The recent studies show that these unusual structures can also be observed when nitrate anions are added [2]. For example, nitrate-containing compounds such as $\text{Pb}_6\text{O}_5(\text{NO}_3)_2$ [3] and $\text{Pb}_2(\text{SeO}_3)(\text{NO}_3)_2$ [4] have a sufficiently high nonlinear optical activity. Despite extensive research, this class of compounds has still been studied very selectively, therefore, currently it is difficult to talk about general trends in the structure formation.

One of the advantages of selenites is their relatively simple and mild synthesis procedures, which is especially relevant for compounds containing thermally unstable anions, in particular nitrates. Solution [5-8] and hydrothermal [9] syntheses are most suitable.

This communication reports the data on a new hydrated lead selenite nitrate: $\text{Pb}_4(\text{SeO}_3)_3(\text{NO}_3)_2 \cdot 2\text{H}_2\text{O}$ (**1**).

¹Institute of Earth Sciences, St. Petersburg State University, St. Petersburg, Russia; *o.siidra@spbu.ru. ²Kola Science Centre, Russian Academy of Sciences, Apatity, Russia. Original article submitted March 10, 2024; revised March 28, 2024; accepted March 28, 2024.

EXPERIMENTAL

Synthesis. The new compound was found as a by-product in the lead selenite synthesis. The solutions containing 20 mmol of lead nitrate and 20 mmol of sodium selenite were heated to boiling and then drained. A heavy, slightly yellowish precipitate immediately formed, which was kept in the mother liquor for approximately 30 min to increase the precipitate crystallinity. A few needle-shaped crystals were found on the precipitate surface after the mother liquor was drained. The second reaction product (sodium nitrate) has a similar morphology, however, the crystals did not dissolve being repeatedly washed with distilled water. One of them was selected for X-ray diffraction (XRD). The yield of crystals of new phase $\text{Pb}_4(\text{SeO}_3)_3(\text{NO}_3)_2 \cdot 2\text{H}_2\text{O}$ can be estimated as ~20%.

The qualitative analysis of $\text{Pb}_4(\text{SeO}_3)_3(\text{NO}_3)_2 \cdot 2\text{H}_2\text{O}$ crystals performed on a scanning electron microscope (Hitachi TM3000) did not reveal any other elements with the atomic number greater than 11 (Na), except Pb and Se.

Single crystal XRD. Single crystal XRD was performed on a Rigaku XtaLAB Synergy-S diffractometer with a PhotonJet-S detector at 120 K. The data were collected with a 0.5° step and a 10 s exposition per frame. The absorption correction was applied taking into account the crystal shape. Crystallographic and structure refinement parameters are given in Table 1. During the structure refinement it is found that OW2, OW3, and OW4 atoms belonging to water molecules are

TABLE 1. Crystallographic and Refinement Parameters of $\text{Pb}_4(\text{SeO}_3)_3(\text{NO}_3)_2 \cdot 2\text{H}_2\text{O}$

Parameter	Data
Crystal system	Triclinic
Space group	$P\bar{1}$
$a, b, c, \text{Å}$	7.2590(2), 7.6454(2), 14.7293(4)
$\alpha, \beta, \gamma, \text{deg}$	84.386(2), 78.311(2), 83.643(2)
$V, \text{Å}^3$	793.18(4)
Radiation	$\text{MoK}\alpha$
$\lambda, \text{Å}$	0.71073
Crystal dimensions, mm	$0.05 \times 0.05 \times 0.20$
Reflections: measured / independent with $F > 4\sigma(F)$	13330 / 3312
R_1	0.031
S	1.03
$\Delta\rho_{\text{min}} / \Delta\rho_{\text{max}}, \text{e/Å}^3$	-2.70 / 2.67
CCDC	2339041

TABLE 2. Calculated BVSs (without taking into account hydrogen bonds) in the Crystal Structure of $\text{Pb}_4(\text{SeO}_3)_3(\text{NO}_3)_2 \cdot 2\text{H}_2\text{O}$

Atom	O1	O2	O3	O4	O5	O6	O7	O8	O9	O10	O11	O12	O13	O14	O15	OW1	OW2*	OW3*	OW4*	$\Sigma_v c$	
Pb1		0.80	0.24	0.34	0.34						0.11	0.09				0.02↓→ 0.02↓	0.07	0.08		2.08	
Pb2	0.39		0.25	0.38		0.24	0.14	0.17	0.10			0.21			0.16						2.05
Pb3	0.29		0.34		0.29	0.29		0.27			0.17			0.13	0.11	0.04↓→ 0.04↓	0.10	0.10		2.12	
Pb4						0.39	0.59	0.30	0.24			0.16	0.16	0.15	0.14						2.13
Se1	1.32	1.28	1.27								0.04						0.03	0.02	0.04	4.00	
Se2				1.31	1.31	1.20						0.03		0.04					0.02	3.90	
Se3							1.32	1.31	1.20				0.06		0.04					3.92	
N1										1.80	1.63	1.55								4.98	
N2													1.83	1.63	1.59					5.05	
$\Sigma_v a$	2.00	2.09	2.10	2.03	1.94	2.11	2.05	2.05	1.54	1.80	1.94	2.03	2.05	1.95	2.05	0.12	0.20	0.18	0.06		

50% site population.

half occupied, while the OW1 position is fully occupied. The calculated bond valence sums (BVSs) are given in Table 2. Practically all calculated BVSs are in good agreement with formal valences of the cations and anions in the structure of **1**. A slightly underestimated BVS value for the O9 atom can be explained by a significant contribution of hydrogen bonds to its valency saturation, which cannot be taken into account at this stage.

CRYSTAL STRUCTURE

The crystal structure of **1** belongs to a new type. The compound crystallizes in the centrosymmetric group $P\bar{1}$. The structure contains four asymmetric lead positions, three selenium positions, two nitrogen positions, and 19 oxygen positions (four of them belong to the oxygen atoms of water molecules). All lead atoms have an irregular coordination environment of oxygen atoms (Fig. 1). The Pb1 atom is coordinated by 11 oxygen atoms at a distance of 2.488(5)–3.535(5) Å. The OW2 and OW3 positions belong to water molecules and are half occupied; Pb2 is surrounded by ten oxygen atoms at a distance of 2.449(5)–3.236(5) Å. The Pb3 coordination consists of 11 oxygen atoms at a distance of 2.508(5)–3.473(5) Å, which include two half occupied OW2 and OW3 positions. It makes the Pb3 environment similar to that of the Pb1 atom. Pb4 is surrounded by ten oxygen atoms at a distance of 2.449(5)–3.196(5) Å. In all coordination polyhedra, a free region can be identified, which indicates the manifestation of the stereochemical activity of the lone pair of the divalent lead cation. All four lead atoms demonstrate different coordination modes to triangular NO₃ groups (Fig. 1). Thus, the Pb1 atom is bidentately bonded only to the N1O₃ group. The Pb2 atom is monodentately coordinated by the N1O₃ group and the N2O₃ triangle. Pb3 has both

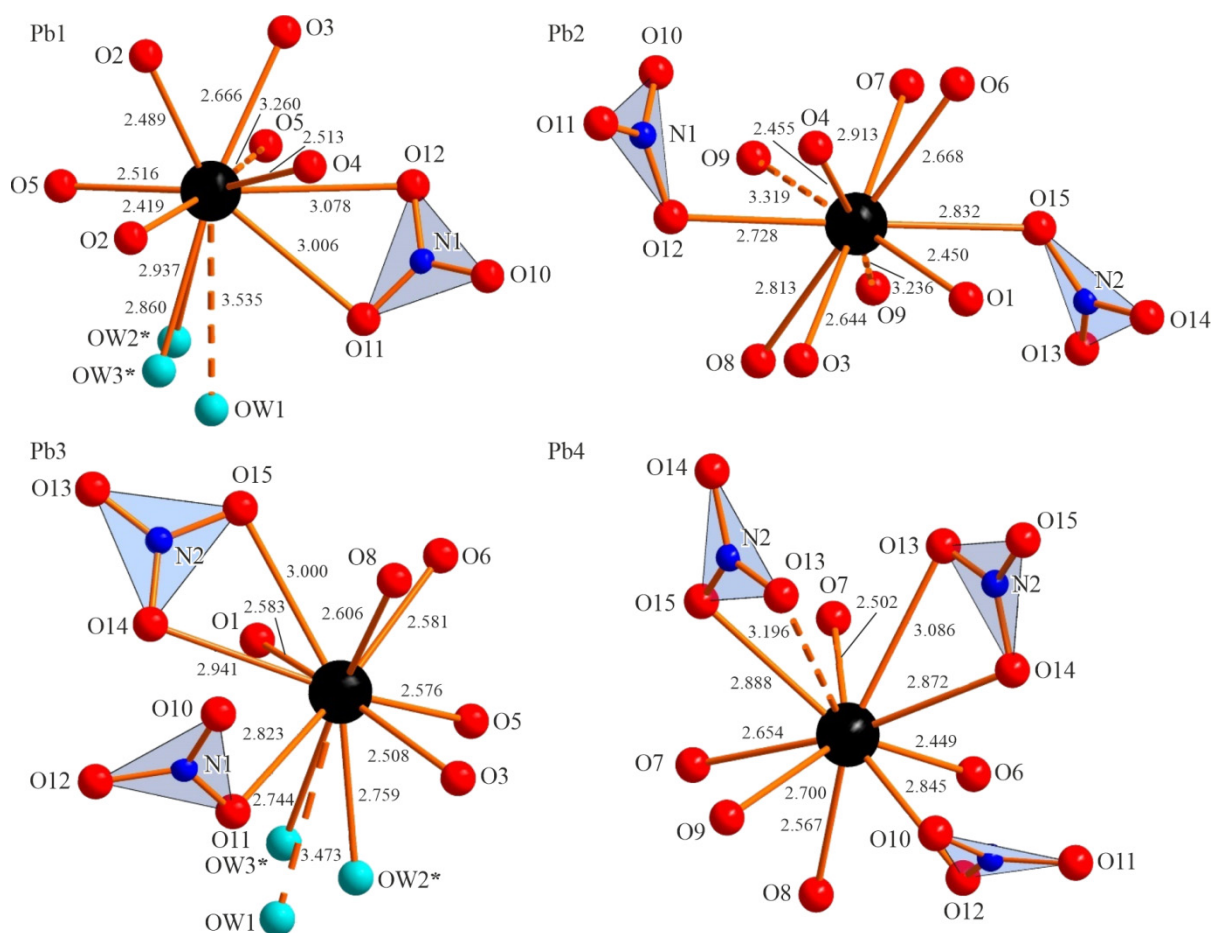


Fig. 1. Coordination environment of Pb1, Pb2, Pb3, and Pb4 atoms in the crystal structure of $\text{Pb}_4(\text{HSeO}_3)_3(\text{NO}_3)_2 \cdot 2\text{H}_2\text{O}$. The OW positions denoted by asterisks are half occupied. The bonds Pb–O > 3.1 Å are shown by dashed lines. All bonds Pb–O ≤ 3.55 Å are shown.

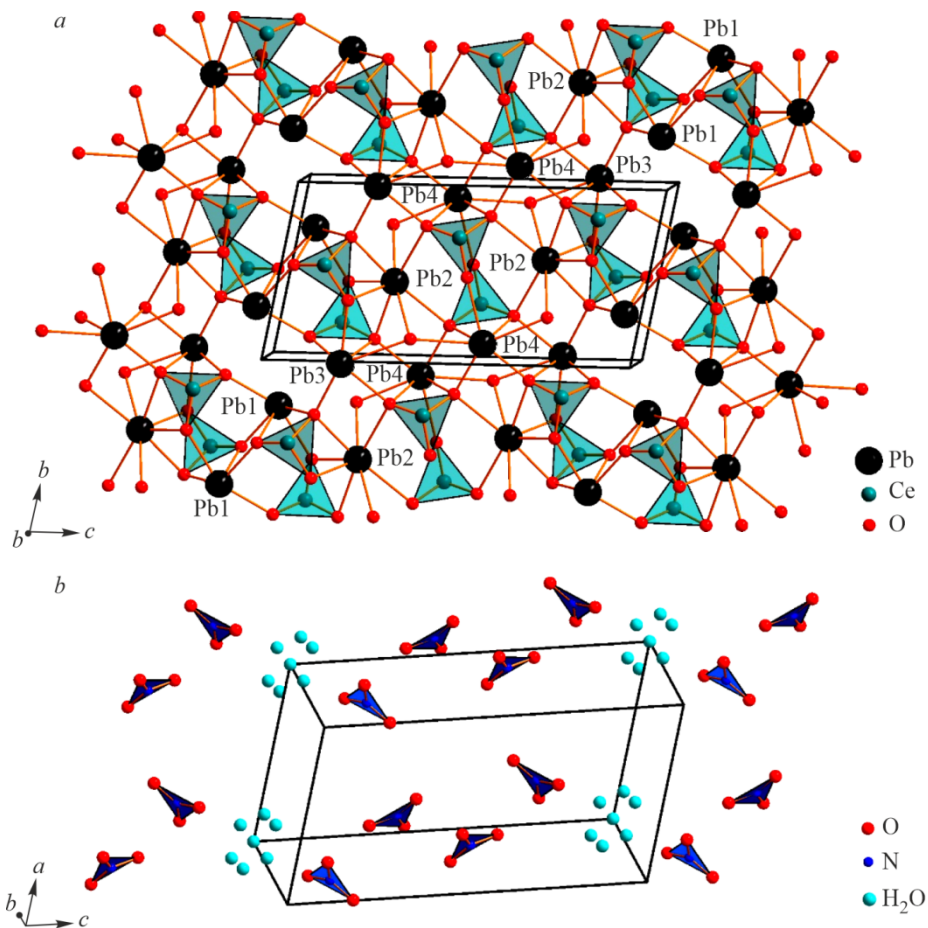


Fig. 2. Structure of **1** can be divided into $[\text{Pb}_4(\text{SeO}_3)_3]^{2+}$ (a) and $\{(\text{NO}_3)_2(\text{H}_2\text{O})_2\}^{2-}$ (b) layers.

types of coordination to two nitrate groups, and the Pb4 atom is coordinated by three NO_3 groups. Valence contributions of each of two OW1–Pb1 bonds and two OW1–Pb3 bonds are ≤ 0.03 v.u. (Table 2). The OW4 water molecule does not make bonds with the cations and is held solely by hydrogen bonds.

Tetravalent selenium forms a classical umbrella SeO_3E group (where E is the lone pair, also with the stereochemical activity). The Se–O distances are different (the difference in bond lengths is 0.02–0.03 Å), which is due to different lead cation environments of selenite oxygen atoms. Taken together, SeO_3^{2-} anions and Pb^{2+} cations form pseudo-layers $[\text{Pb}_4(\text{SeO}_3)_3]^{2+}$, with nitrate anions and water molecules being located between them (Fig. 2). The nitrate anions and water molecules complete the coordination of lead located in a covalent layer. Stereochemically active electron pairs of SeO_3E groups are directed toward each other (Fig. 3), forming special cavities (channels) called micelles [10].

DISCUSSION

New $\text{Pb}_4(\text{SeO}_3)_3(\text{NO}_3)_2 \cdot 2\text{H}_2\text{O}$ is the second lead selenite nitrate compound after the anhydrous $\text{Pb}_2(\text{SeO}_3)(\text{NO}_3)_2$ compound described in [4]. It is noteworthy that both selenite nitrates were prepared from aqueous solutions, but under different conditions. $\text{Pb}_2(\text{SeO}_3)(\text{NO}_3)_2$ as well as its phosphite analogue $\text{Pb}_2(\text{HPO}_3)(\text{NO}_3)_2$ is formed under the action of selenious acid on a diluted solution of lead nitrate (the medium is slightly acidic), while $\text{Pb}_4(\text{SeO}_3)_3(\text{NO}_3)_2 \cdot 2\text{H}_2\text{O}$ was obtained in the interaction of solid lead selenite with an excess of a NaNO_3 solution (possibly, containing a small excess of $\text{Pb}(\text{NO}_3)_2$; the medium is nearly neutral). In our case, a hot solution with sufficiently high concentrations of nitrate ions interacts with

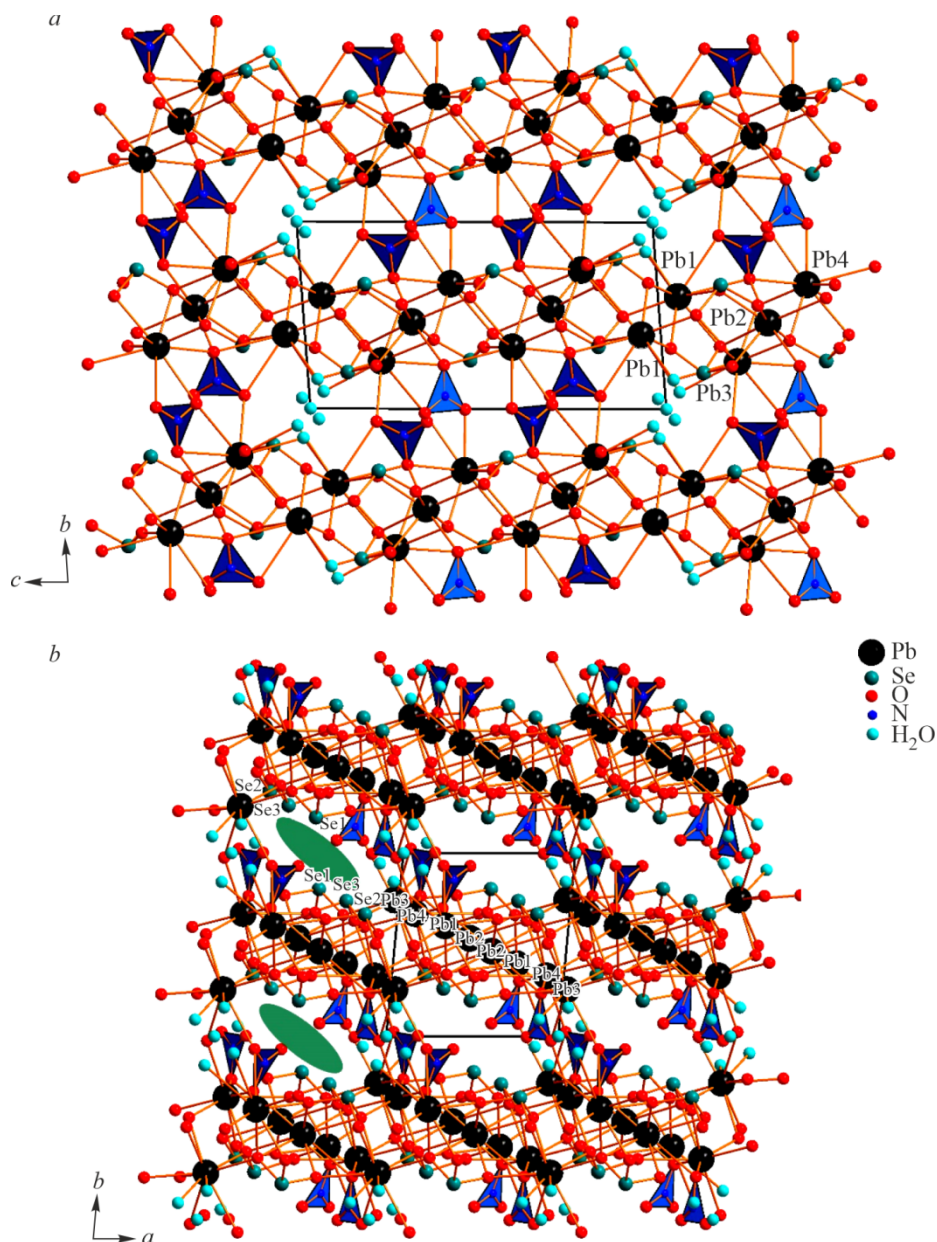


Fig. 3. General projection of the crystal structure of $\text{Pb}_4(\text{SeO}_3)_3(\text{NO}_3)_2 \cdot 2\text{H}_2\text{O}$ along the a (a) and c (b) axes. Micelles are shown by green ovals.

the solid phase containing selenite anions. It can be assumed that due to a relatively high temperature and the ionic strength of the concentrated NaNO_3 solution, a partial dissolution of lead selenite occurs followed by crystallization of **1**.

The structures of anhydrous $\text{Pb}_2(\text{SeO}_3)(\text{NO}_3)_2$ and **1** can be described as porous frameworks (Fig. 3). Different architectures are explained by the presence of additional water molecules and different $\text{Pb}^{2+}:\text{SeO}_3^{2-}$ ratios. Anhydrous selenite nitrate with a more complicated composition $\text{Pb}_2\text{Cu}_3\text{O}_2(\text{NO}_3)_2(\text{SeO}_3)_2$ [11] is also known, in which the primary structural blocks are CuO_4 squares sharing vertices to form a zigzag chain surrounded by lead cations and selenite groups on both sides. In this case, selenium and lead lone pairs are directed to the interlayer space, which indicates the presence of the chemical scissors effect.

The structural similarity of nitrates with halides can be seen when comparing these structures with the $\text{Pb}_8\text{Cu}^{2+}(\text{SeO}_3)_4\text{Br}_{10}$ compound [12] obtained by the chemical gas transport reaction as a by-product in the synthesis of the

sarrabusite bromide analogue [13]. Although this structure has a chain motif, it is formed similar to $\text{Pb}_2\text{Cu}_3\text{O}_2(\text{NO}_3)_2(\text{SeO}_3)_2$ around copper atoms and is lined by lone pairs pushing halogen to the interlayer space.

The role of water as a factor contributing to a decrease in the structure dimensionality can also be illustrated by the example of favreauite mineral $\text{PbBiCu}_6\text{O}_4(\text{SeO}_3)_4(\text{OH})(\text{H}_2\text{O})$ [14]. In this structure, copper selenite layers are highly corrugated, and the voids contain disordered water molecules that are relatively weakly bonded with strong covalent layers and fill the free space.

Therefore, a combination of low valent cations of metals and non-metals with the oxygen environment results in the formation of interfaces lined by stereochemically active lone pairs. On the other side of these interfaces, rigid anions weakly interacting with low valent cations are located, which determines the chemical scissors effect. This effect is apparently strengthened by water molecules forming only relatively weak hydrogen bonds and also contributing to a decrease in the density and/or dimension of covalently bonded frameworks.

ACKNOWLEDGMENTS

The single crystal XRD study was performed using the equipment of the X-ray Diffraction Research Resource Center of the St. Petersburg State University.

The authors are grateful to E. L. Belokoneva and an anonymous reviewer for valuable comments and suggestions that helped us to improve this article.

FUNDING

This work was supported by ongoing institutional funding. No additional grant to carry out or direct this particular research were obtained.

CONFLICT OF INTERESTS

The authors of this work declare that they have no conflicts of interest.

REFERENCES

1. H. Yu, N. Z. Koocher, J. M. Rondinelli, and P. S. Halasyamani. $\text{Pb}_2\text{BO}_3\text{I}$: a borate iodide with the largest second-harmonic generation (SHG) response in the $\text{KBe}_2\text{BO}_3\text{F}_2$ (KBBF) family of nonlinear optical (NLO) materials. *Angew. Chem., Int. Ed.*, **2018**, 57(21), 6100-6103. <https://doi.org/10.1002/anie.201802079>
2. A. H. Reshak. Lead nitrate hydroxide: A strong second-order optical nonlinearity acentric crystal with high laser damage thresholds. *J. Appl. Phys.*, **2016**, 119(10). <https://doi.org/10.1063/1.4943650>
3. D. O. Charkin, A. S. Borisov, I. V. Plokhikh, S. Y. Stefanovich, A. I. Zadoya, A. N. Zaloga, T. F. Semenova, and O. I. Siidra. $\text{Pb}_6\text{O}_5(\text{NO}_3)_2$: a nonlinear optical oxynitrate structurally based on lead oxide framework. *Inorg. Chem.*, **2020**, 59(6), 3523-3526. <https://doi.org/10.1021/acs.inorgchem.0c00001>
4. C.-Y. Meng, L. Geng, W.-T. Chen, M.-F. Wei, K. Dai, H.-Y. Lu, and W.-D. Cheng. Syntheses, structures, and characterizations of a new second-order nonlinear optical material: $\text{Pb}_2(\text{SeO}_3)(\text{NO}_3)_2$. *J. Alloys Compd.*, **2015**, 640, 39-44. <https://doi.org/10.1016/j.jallcom.2015.04.021>
5. V. Y. Grishaev, O. I. Siidra, M. R. Markovski, D. O. Charkin, T. A. Omelchenko, and E. V. Nazarchuk. Synthesis and crystal structure of two novel polymorphs of $(\text{NaCl})[\text{Cu}(\text{HSeO}_3)_2]$: a further contribution to the family of layered copper hydrogen selenites. *Z. Kristallogr. - Cryst. Mater.*, **2023**, 238(5/6), 177-185. <https://doi.org/10.1515/zkri-2023-0004>

6. D. O. Charkin, V. Y. Grishaev, T. A. Omelchenko, E. V. Nazarchuk, S. Y. Stefanovich, and O. I. Siidra. $\text{KNO}_3 \cdot 3\text{H}_2\text{SeO}_3$ and $\text{NaHSeO}_3 \cdot 3\text{H}_2\text{SeO}_3$: Two non-centrosymmetric co-crystals. *Solid State Sci.*, **2023**, *137*, 107116. <https://doi.org/10.1016/j.solidstatesciences.2023.107116>
7. D. O. Charkin, V. Y. Grishaev, A. S. Borisov, P. A. Chachin, E. V. Nazarchuk, and O. I. Siidra. A nonpolar bond to hydrogen vs. lone pair: Incorporation of HPO_3^{2-} and SeEO_3^{2-} into a lead perhenate framework. *J. Solid State Chem.*, **2023**, *318*, 123706. <https://doi.org/10.1016/j.jssc.2022.123706>
8. D. O. Charkin, E. V. Nazarchuk, D. N. Dmitriev, V. Y. Grishaev, T. A. Omelchenko, D. V. Spiridonova, and O. I. Siidra. Protonated organic diamines as templates for layered and microporous structures: Synthesis, crystal chemistry, and structural trends among the compounds formed in aqueous systems transition metal halide or nitrate–diamine–selenious acid. *Int. J. Mol. Sci.*, **2023**, *24*(18), 14202. <https://doi.org/10.3390/ijms241814202>
9. P. M. Almond and T. E. Albrecht-Schmitt. Hydrothermal syntheses, structures, and properties of the new uranyl selenites $\text{Ag}_2(\text{UO}_2)(\text{SeO}_3)_2$, $\text{M}[(\text{UO}_2)(\text{HSeO}_3)(\text{SeO}_3)]$ ($\text{M} = \text{K}, \text{Rb}, \text{Cs}, \text{Tl}$), and $\text{Pb}(\text{UO}_2)(\text{SeO}_3)_2$. *Inorg. Chem.*, **2002**, *41*(5), 1177-1183. <https://doi.org/10.1021/ic0110732>
10. E. Makovicky. Modular and crystal chemistry of sulfosalts and other complex sulfides. In: *Modular Aspects of Minerals: EMU Notes in Mineralogy, Vol. 1* / Ed. S. Merlino. Budapest, Hungary: European Mineralogical Union, **1997**, 237-271. <https://doi.org/10.1180/emu-notes.1.8>
11. H. Effenberger. $\text{PbCu}_3(\text{OH})(\text{NO}_3)(\text{SeO}_3)_3 \cdot 0.5\text{H}_2\text{O}$ and $\text{Pb}_2\text{Cu}_3\text{O}_2(\text{NO}_3)_2(\text{SeO}_3)_2$: Synthesis and crystal structure. *Monatsh. Chem.*, **1986**, *117*(10), 1099-1106. <https://doi.org/10.1007/bf00811322>
12. O. I. Siidra, V. Y. Grishaev, E. V. Nazarchuk, and R. A. Kayukov. Three new copper-lead selenite bromides obtained by chemical vapor transport: $\text{Pb}_5\text{Cu}^+_4(\text{SeO}_3)_4\text{Br}_6$, $\text{Pb}_8\text{Cu}^{2+}(\text{SeO}_3)_4\text{Br}_{10}$, and the synthetic analogue of the mineral sarrabusite, $\text{Pb}_5\text{Cu}^{2+}(\text{SeO}_3)_4(\text{Br},\text{Cl})_4$. *Mineral. Petrol.*, **2023**, *117*(2), 281-291. <https://doi.org/10.1007/s00710-023-00825-2>
13. M. Gemmi, I. Campostrini, F. Demartin, T. E. Gorelik, and C. M. Gramaccioli. Structure of the new mineral sarrabusite, $\text{Pb}_5\text{CuCl}_4(\text{SeO}_3)_4$, solved by manual electron-diffraction tomography. *Acta Crystallogr., Sect. B: Struct. Sci.*, **2012**, *68*(1), 15-23. <https://doi.org/10.1107/s010876811104688x>
14. S. J. Mills, A. R. Kampf, A. G. Christy, R. M. Housley, B. Thorne, Y.-S. Chen, and I. M. Steele. Favreauite, a new selenite mineral from the El Dragón mine, Bolivia. *Eur. J. Mineral.*, **2014**, *26*(6), 771-781. <https://doi.org/10.1127/ejm/2014/0026-2405>

Publisher's Note. Pleiades Publishing remains neutral with regard to jurisdictional claims in published maps and institutional affiliations.